Tensile behaviour of submicrocrystalline ferritic steel processed by large-strain deformation

A. Belyakov[ab]*, K. Tsuzaki[bc], Y. Kimura[c] and Y. Mishima[c]

[a]*Belgorod State University, Koroleva 2a, Belgorod 308034, Russia;* [b]*Structural Metals Center, National Institute for Materials Science, Sengen 1-2-1, Tsukuba, Ibaraki 305-0047, Japan;* [c]*Interdisciplinary Graduate School of Science and Engineering, Tokyo Institute of Technology, Nagatsuta 4259, Midori, Yokohama 226-8502, Japan*

Mechanical tests have been carried out on Fe–15%Cr ferritic stainless steel with various microstructures. Ultrafine-grained microstructures with grain sizes of 0.2–0.3 μm were developed by large-strain cold-working and light annealing. The effects of severe deformation on the mechanical behaviour of as-processed and recovered steel were evaluated with reference to the same material having conventional work-hardened and recrystallised microstructures. Despite the low dislocation density in the fine grain interiors in the as-processed state, the samples with strain-induced submicrocrystalline structure were characterised by high internal stresses that resulted in a higher strength than could be expected from simple grain-size strengthening. These internal stresses were associated with a non-equilibrium state of strain-induced grain boundaries after severe deformation.

Keywords: severe deformation; submicrocrystalline alloys; grain boundaries; tensile testing; strengthening mechanisms; recovery

1. Introduction

Over the past decade, submicrocrystalline metals and alloys with grain sizes ranging from tens to hundreds of nanometres have attracted widespread attention among materials scientists [1–6]. Such structural materials are thought to have a beneficial combination of mechanical properties, i.e. high strength and sufficiently large ductility. One of the most promising methods for obtaining submicrocrystalline structures is by severe deformation. Several processing techniques have been developed to achieve the required large strains at relatively low temperatures [3,4,6–10]. The evolution mechanism of submicrocrystalline structures has also been documented [3,6,9,11–13]. Upon severe deformation, the ultrafine-grained structures result from a gradual increase in angular misorientations between deformation subgrains with an increase in strain. The formation of high-angle strain-induced grain boundaries is accompanied by a decrease in dislocation densities in the interiors of fine (sub)grains. Nevertheless, the submicrocrystalline materials processed

*Corresponding author. Email: belyakov@bsu.edu.ru

by large-strain plastic working are characterised by a high level of residual stresses, which are probably associated with a non-equilibrium state of strain-induced grain boundaries.

In contrast to the structural mechanisms operating during large-strain deformation, the mechanical properties of submicrocrystalline metals and alloys have not, as yet, been studied in detail. The effect of high internal stresses on the mechanical behaviour of ultrafine-grained materials processed by severe deformation is still unclear due to the lack experimental data. The specific experimental methods for severe deformations at low homologous temperatures only enable cold-working to relatively small strains or the processing of samples up to a certain size, which is sufficient for structural investigations but rather small for carrying out standard mechanical tests. Recently, some conventional processing methods of metal working, i.e. rolling and swaging, were successfully utilised for severe deformation in the development of submicrocrystalline structure in large-scale samples [14,15]. The structural changes were shown to follow the general sequence of microstructure evolution upon severe deformation that commonly leads to ultrafine-grain formation after sufficiently large strains.

The aim of the present work was to clarify the mechanical behaviour of samples with submicrocrystalline structures developed by large-strain deformation. In particular, this study focused on the effect of internal stresses that evolved by severe deformation on the strength of material and the softening consequences of recovery annealing with reference to the same alloy cold-worked to a conventional strain level. An Fe–15%Cr steel was chosen as a typical representative of a wide grade of single-phase metals and alloys.

2. Experimental procedure

A ferritic stainless steel, Fe–0.003C–0.01Mn–0.001P–0.001S–15.0Cr–0.003N (all in mass%), was selected as the starting material. The steel was vacuum-melted and cast into a 20-kg ingot followed by homogenisation and hot-rolling to 21.3×21.3 mm square bars. The processing details are outlined elsewhere [15]. Large-strain cold-working was carried out by bar rolling to 7.8×7.8 mm square bars followed by swaging from a diameter of Ø7.0–Ø1.95 mm. A total strain of 4.6 was obtained. Part of the hot-rolled material was cold-rolled to 12.9×12.9 mm square bars to obtain reference samples processed to a relatively small strain of 1.0. The subsequent annealing treatment of the cold-worked samples was conducted in an argon atmosphere at temperatures of 400–650°C.

Structural observations were performed on longitudinal and transverse sections using a JEM-2010F transmission electron microscope (TEM) operating at 200 kV. The TEM specimens were prepared by the double-jet electro-polishing method using a 5% solution of perchloric acid in glacial acetic acid. Grain/subgrain sizes were measured on the TEM micrographs by the linear-intercept method, including those at all clear visible (sub)boundaries. The dislocation density was measured by counting the individual dislocations in grain/subgrain interiors on at least six arbitrarily selected typical TEM images for each sample. Tensile tests were carried out on two sets of samples that were cold-worked to total strains of 1.0 and 4.6. The tensile axis was parallel to the rolling/swaging axis. Rectangular specimens with a thickness of 1 mm, a width of 3 mm and a gauge length of 12 mm were machined from the samples strained to 1.0. The circular specimens were fabricated from the samples strained to 4.6 by bonding the ends of the

60-mm sample rods (Ø1.95 mm) with epoxy cement, and leaving an 8-mm gauge length in the centre portion. This assembly was electro-polished in the same solution used for preparation of TEM thin foils. Tensile testing was performed at an ambient temperature on a Shimadzu AG-10TE testing machine at a strain rate of about 10^{-3} s.

3. Results

3.1. *Deformation microstructures*

Strain levels of $\varepsilon = 1.0$ and $\varepsilon = 4.6$ were selected for the present comparative study. Typical deformation microstructures are shown in Figures 1 and 2. After a relatively small strain of 1.0, which is the conventional strain level applied in metalworking processes, the deformation microstructure consisted of well-developed cell blocks, which are separated by dense dislocation walls (Figure 1). This is a typical cold-worked microstructure with high dislocation density. The average dislocation density in the subgrain interiors is $(5.6 \pm 0.7) \times 10^{14}\,\mathrm{m}^{-2}$; the average subgrain size, measured in the transverse direction relative to the rolling axis, is ~310 nm.

On the other hand, the samples processed to a large total strain of 4.6 are characterised by a ribbon-like deformation microstructure with fine grains/subgrains, which are highly elongated in the direction of metal flow (Figure 2a). The average transverse size of these (sub)grains is ~210 nm and the fraction of high-angle (sub)boundaries comprises about 0.66, which was evaluated by orientation imaging microscopy [15]. Note that the (sub)grains developed by severe deformation include a smaller number of dislocations in their interiors compared to those subject to conventional strain. The interior dislocation density is $(2.9 \pm 0.6) \times 10^{14}\,\mathrm{m}^{-2}$ after cold-working to a strain of 4.6. However, despite the relatively low dislocation density, the (sub)grains in these samples possess large

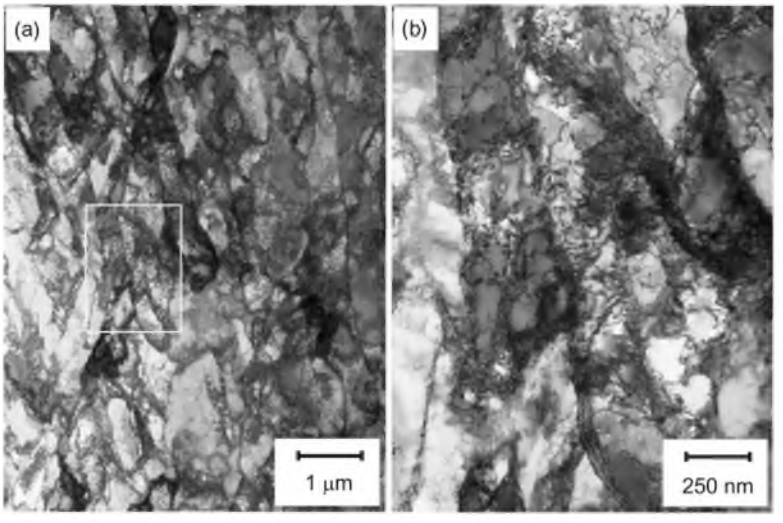

Figure 1. Deformation microstructures in Fe–15%Cr steel after cold-rolling to a total strain of 1.0. Micrograph in (b) represents the selected portion of (a). The rolling axis is vertical in the micrographs.

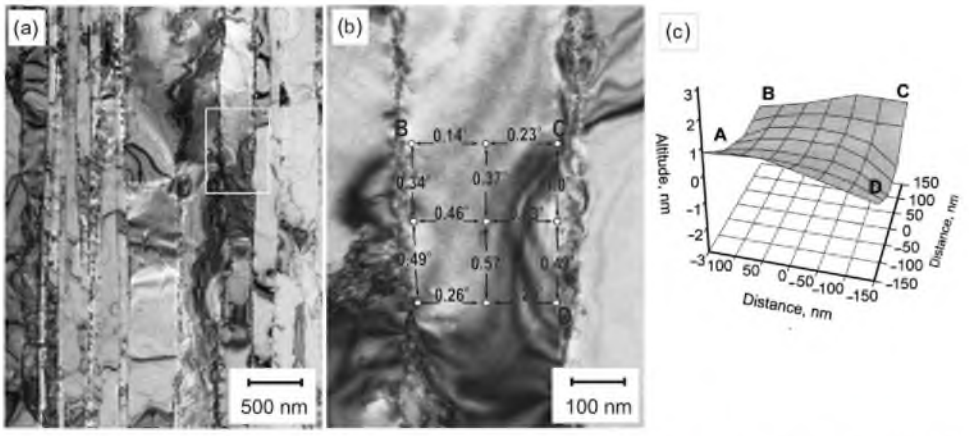

Figure 2. Deformation microstructure in Fe–15%Cr steel after cold-working to a total strain of 4.6. Numbers in (b) indicate the local disorientations in degrees between the pointed micro-regions. The surface in (c) illustrates the bent lattice plane within the selected area of A–B–C–D shown in (b). The rolling/swaging axis is vertical in the micrographs.

internal distortions, as evident from the numerous bend contours and clearly visible on the TEM image of the large-strained microstructure. Some of the bend contours cross over the (sub)grains and terminate at the (sub)grain boundaries, while others look like semi-loops located near the boundaries. An example of the latter is represented in Figure 2b as an enlarged image of the selected portion in Figure 2a. The points in Figure 2b indicate the areas where the orientations of the crystal lattice were precisely evaluated by the convergent beam Kikuchi diffraction technique. The numbers between the points indicate the local disorientations or the curvatures of the grain lattice.

The selected grain in Figure 2b is completely free of any dislocations in its interior. However, the crystal lattice of this grain is bent at large angles. The local curvatures attain 1° over a distance of 150 nm near the boundary. The lattice curvature of this grain is illustrated more clearly by the bent surface in Figure 2c. The relative altitudes of the surface of the area outlined by A–B–C–D were plotted as deviations of the central electron spots in Kikuchi maps from that of the grain centre with an altitude of zero. According to the diffraction conditions, this surface may be considered as a crystallographic plane of {1 1 1}. The selected grain portion is characterised by a saddle-shaped lattice curvature. The distortions are more pronounced in the vicinity of the grain boundary, suggesting that the complex elastic strains develop in the fine grains after large-strain deformation; therefore, high internal stresses are maintained by the strain-induced grain boundaries.

Assuming that the elastic strain in a bent lattice changes linearly with respect to the thickness of the foil specimen with a zero point in the middle plane, the elastic normal strain ε and the shear strain γ can be evaluated as follows [16]: $\varepsilon = t'\theta_\varepsilon/d$ and $\gamma = t'\theta_\gamma/d$, where d is the distance between the measured points, t' is the distance from the midpoint of the specimen thickness, t, (i.e. $0 < t' < 0.5t$), and θ_ε and θ_γ are the rotation angles responsible for the normal and shear strains, respectively. Generally, the angular disorientation, θ, between any two points within a grain includes θ_ε and θ_γ with the same probability [16]. Therefore, the values of both θ_ε and θ_γ can be roughly related to the

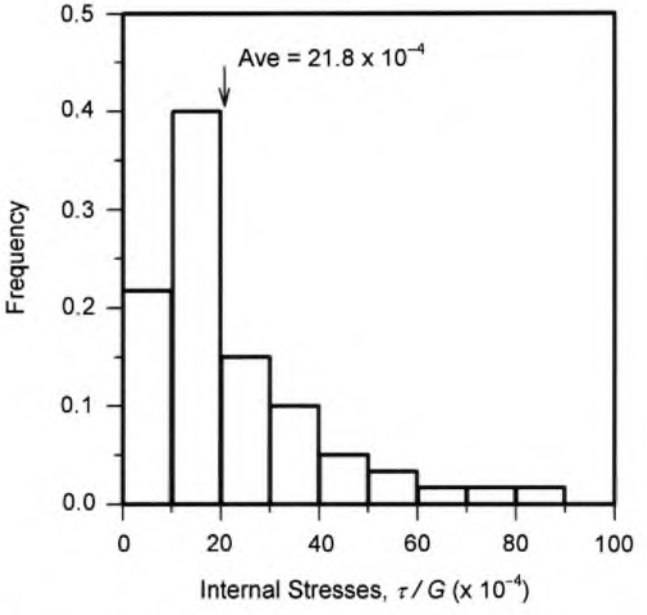

Figure 3. Distribution of internal stresses in Fe–15%Cr steel processed by cold-working to a total strain of 4.6. The stresses were evaluated by Equation (1).

value of the measured angular disorientation, as $\theta_\varepsilon \approx \theta_\gamma \approx 0.7\theta$. Then, the residual shear stresses τ, associated with the maximal value of the elastic distortions, can be derived as follows:

$$\frac{\tau}{G} = \frac{0.35t\theta}{d}, \tag{1}$$

where G is the shear modulus and t is the specimen thickness. Figure 3 shows the quantitative analysis of the internal stresses, which were evaluated by Equation (1), in 60 different regions of 12 different fine grains. The distribution of internal stresses shows a rather sharp peak at $15 \times 10^{-4} G$, while the maximum stress approaches $10^{-2} G$. The average internal stress is $21.8 \times 10^{-4} G$. Such large internal stresses may significantly alter the mechanical behaviour of submicrocrystalline materials processed by severe deformation compared to samples with unstressed microstructures after some recovery treatment.

Annealing at relatively low temperatures below 500°C does not lead to any significant changes in the deformation microstructures, i.e. grain/subgrain size and density of dislocations in (sub)grain interiors (Tables 1 and 2). The microstructures annealed at 400°C for 30 min (Figure 4) resemble those in the as-processed states. In the samples cold-worked to a relatively small strain of 1.0, the high dislocation density is hardly reduced and the subgrain size of about 300 nm does not coarsen after such low-temperature annealing. Similarly, the annealed microstructures in samples subjected to a large strain of 4.6 are characterised by highly elongated grains/subgrains with a transverse size of about 230 nm and interior dislocation density of about $3 \times 10^{14}\,\mathrm{m}^{-2}$ – values that are almost identical with

Table 1. Transverse subgrain/grain size, dislocation density in (sub)grain interiors and some mechanical properties of Fe–15%Cr steel cold-worked to a total strain of 1.0 and then annealed under various conditions.

Processing conditions	Subgrain or grain size (μm)	Dislocation density (10^{14} m^{-2})	Offset yield strength ($\sigma_{0.2}$, MPa)	Tensile strength (σ_B, MPa)	Total elongation (δ, %)
As-processed	0.31	5.6	392	718	10.3
400°C, 30 min	0.30	6.0	486	679	12.5
500°C, 30 min	0.32	5.2	485	648	15.3
600°C, 30 min	0.33	4.8	430	591	18.9
650°C, 8 h	18.0	–	172	350	63.3

Table 2. Transverse grain/subgrain size, dislocation density in (sub)grain interiors and some mechanical properties of Fe–15%Cr steel cold-worked to a total strain of 4.6 and then annealed under various conditions.

Processing conditions	Grain/subgrain size (μm)	Dislocation density (10^{14} m^{-2})	Offset yield strength ($\sigma_{0.2}$, MPa)	Tensile strength (σ_B, MPa)	Total elongation (δ, %)	Reduction of area (ψ, %)
As-processed	0.21	2.9	896	1088	11.0	64
400°C, 30 min	0.23	3.2	643	988	11.6	73
500°C, 30 min	0.26	2.5	570	839	15.4	80
500°C, 2 h	0.27	2.8	593	794	15.0	78
500°C, 8 h	0.32	2.6	579	779	16.9	79
600°C, 30 min	0.40	2.7	465	640	24.0	85
650°C, 1 h	1.02	0.2	347	534	39.4	86
650°C, 8 h	3.97	–	262	453	35.0	87

those in the cold-worked state. An increase in annealing temperature results in the development of recrystallisation processes. In the same material, primary (discontinuous) recrystallisation was shown to take place in conventionally strained samples after heating above 600°C, when recrystallising grains nucleated and expanded, consuming the cold-worked substructures [17]. In the severely deformed samples, recrystallisation develops in a continuous manner, i.e. the strain-induced submicrocrystalline structures gradually coarsen during annealing at temperatures of $T \geq 500$°C [17]. Such annealing behaviour allows us to obtain a wide variety of grain sizes, ranging from 200 nm to normally recrystallised grains.

3.2. *Mechanical behaviour*

Two sets of flow curves obtained by tensile tests for the samples cold-worked to strains of 1.0 and 4.6 and then annealed under various conditions are shown in Figure 5. The true flow stresses were evaluated by assuming a uniform reduction in the cross-sections of the specimens according to the tensile strains during the tests. Some mechanical properties of

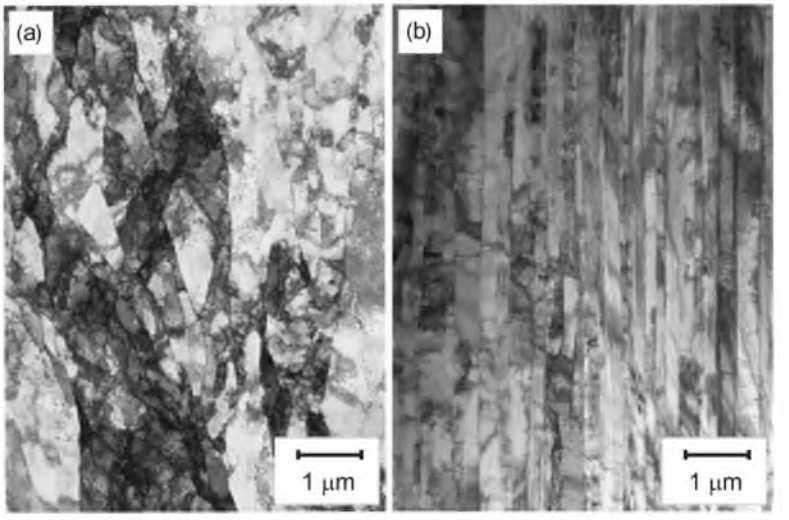

Figure 4. Recovered microstructures in Fe–15%Cr steel after annealing at 400°C for 30 min following cold-working to total strains of 1.0 (a) and 4.6 (b).

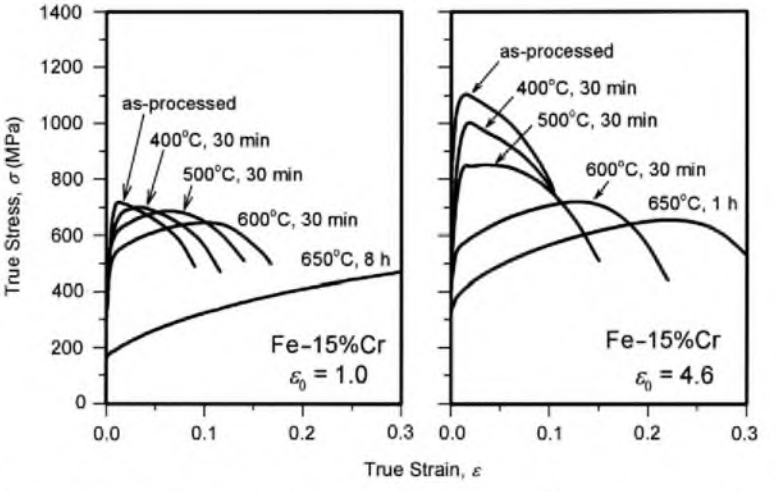

Figure 5. Deformation behaviour during tensile tests for Fe–15%Cr steel processed by cold-working to total strains of $\varepsilon_0 = 1.0$ and $\varepsilon_0 = 4.6$ and then annealed under indicated conditions.

these samples, along with the transverse grain/subgrain sizes and dislocation density in (sub)grain interiors, are shown in Tables 1 and 2. The mechanical properties displayed in Figure 5 and Tables 1 and 2 were averaged over three tensile specimens. The larger strained samples are characterised by higher levels of flow stresses and strengths, while ductility does not depend on the cold-strain, at least under the present experimental conditions. The samples processed by cold-rolling/swaging to a total strain of 4.6 show a large reduction in area, which is comparable to that of the well-annealed samples.

The flow stress level commonly decreases with an increase in annealing temperature. Figure 5 shows that the annealing effect depends significantly on the preceding cold strain. Annealing for 30 min at temperatures of 400–600° resulted in a partial recovery of the cold-worked microstructures in the samples subjected to cold-rolling with a total strain of 1.0. The recovered samples have lowered flow stresses and expanded elongation compared to those subjected to cold-working. This difference between the strained and recovered samples increases with annealing temperature; however, the recovery treatment does not provide as dramatic a change as recrystallisation. The fully recrystallised microstructure was obtained by annealing at 650°C for 8 h. All the flow curves for cold-worked and recovered samples are located at almost the same level of ~600 MPa, which is significantly higher then the flow curve of the recrystallised sample. Moreover, the offset yield strength may even be increased by recovery annealing of the samples processed to conventional strain (Table 1).

In contrast, annealing treatments in the same temperature range of 400–600°C resulted in a significant deterioration in strength properties of the samples, which were previously cold-worked to a large strain of 4.6 (Figure 5 and Table 2). The increase in annealing temperature leads to a gradual decrease in the flow stresses down to those of the well recrystallised samples with relatively coarse grained microstructures. Note that the high-strength properties of the large-strained sample can be lowered substantially by light annealing at 400°C, although the grain size and the interior dislocation density are almost unchanged. This suggests that the strength properties of submicrocrystalline materials that developed by severe deformation are affected not only by a grain size and interior dislocation density, but by some other structural features such as high residual stresses.

4. Discussion

The development of high internal stresses that accompanies the evolution of submicrocrystalline structures during severe deformation was shown to be responsible for the decrease in dislocation density in fine grain interiors [18]. The internal stresses provide a back-force acting on the moving dislocation that pushes the dislocation out to its original source when the applied load is released. The high internal stresses in the studied material after large strain are probably associated with an inhomogeneous distribution of misfit grain boundary dislocations, which are reaction products of dislocation fluxes crossing over the neighbouring grains. Any extrinsic grain boundary dislocations produce long-range stress fields [19]. These internal stresses, which evolved during unidirectional deformation, should further retard plastic flow in the same direction. Therefore, an analogous interaction between dislocations and residual stresses, should be taken into account when considering the mechanical behaviour of submicrocrystalline materials. Upon loading, the moving dislocation should overcome the additional back-force from the residual stresses that result in the extra strengthening of ultrafine-grained samples subjected to severe deformation.

Considering the wedge disclination at a grain boundary as the source of high internal stresses, the maximal back-stresses τ_B acting on a lattice dislocation crossing over the grain interior can be expressed as follows [18,20]:

$$\tau_B = \frac{G\omega}{4\pi(1-\nu)}, \tag{2}$$

where ω is the Frank vector (or the rotation vector characterising the power of disclination) and ν is Poisson's ratio. Strictly speaking, a disclination is a kind of virtual defect. In a real lattice, the wedge disclination at a grain boundary can be represented by a local excess of grain boundary dislocations. Then, the power of the wedge disclination equals the angular rotation, which is created by the array of excess dislocations, i.e. $\omega = b/l$, where b is the Burgers vector and l is the spacing between the excess dislocations. The accumulation of excess dislocations at grain boundaries during large-strain deformation seems to be a recovery-controlled process, similar to the size of deformation cells or subgrains. It is worthwhile relating the density of excess dislocations at (sub)boundaries in submicrocrystalline materials to the inverse grain/subgrain size (D); thus, $l = D/N$. To a first approximation, the factor of N can be considered as the total number of excess dislocations that are involved at a grain boundary. Therefore, the residual back-stresses acting on lattice dislocations can be represented as a function of the grain size:

$$\tau_B = \frac{GNb}{4\pi(1-\nu)}\frac{1}{D}. \tag{3}$$

The mechanical properties of ultrafine-grained materials are mainly determined by the grain size strengthening according to the Hall–Petch relationship, which is valid for various recrystallised metals and alloys [21–24]. However, the conventional Hall–Petch relation frequently does not fit experimental data well over a wide range of grain sizes, including submicrocrystalline structures [25–27]. On the other hand, the above considerations provide a way for expanding the Hall–Petch relationship to consider the effect of internal stresses that develop in submicrocrystalline structures upon processing by large-strain deformation. Since the internal stresses induce the resistance for dislocation motion caused by long-range elastic interactions, they can be accounted for by including an additional term in the Hall–Petch relationship. Therefore, the modified expression for the offset yield strength ($\sigma_{0.2}$) includes three terms:

$$\sigma_{0.2} = \sigma_0 + \sigma(D^{-1}) + \sigma(D^{-0.5}). \tag{4}$$

The first and third terms are those from the standard relationship, and the second term represents the additional strengthening that comes from internal stresses, which can be expressed as an inverse proportion to the grain size (Equation (3)). Taking the value of internal stresses of $2 \times 10^{-3} G$ (Figure 3), $D = 0.21\,\mu m$ (Table 2) and $G = 6.4 \times 10^4$ MPa [28], Equation (3) can be written as $\tau_B = 27D^{-1}$ MPa μm for the studied material. Then, the second term in Equation (4) is $\sigma(D^{-1}) = 2\tau_B D^{-1} = 54D^{-1}$ MPa μm.

The experimental relationship between the offset yield stress and the grain size is shown in Figure 6. Some data from the literature [10,23,29] are also included in the figure for reference. Note here that Tsuji et al. [10] obtained ultrafine-grained samples from interstitial-free steel by accumulative roll-bonding at 400°C followed by annealing at various temperatures. The strength of the ultrafine-grained samples processed by severe deformation coincides with that predicted by Equation (4) (at least for the present experimental conditions when the tensile axis is aligned with the flow direction during processing), while the annealed samples obey the conventional form of the Hall–Petch relationship. The effect of residual stresses on the strength of strain-induced

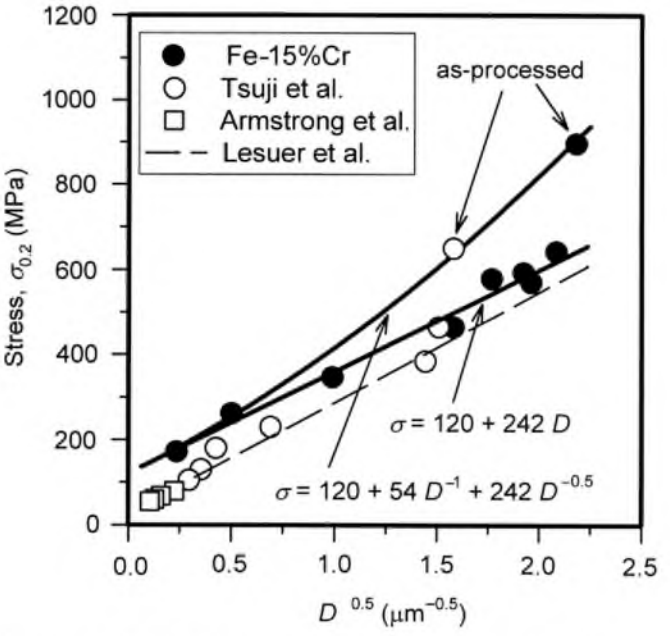

Figure 6. Effect of the grain size on the offset yield strength for Fe–15%Cr steel along with selected reference data for various steels [10,23,29].

submicrocrystalline materials increases with decreasing grain size. In the range of relatively large grain sizes above 1 μm, the influence of internal stresses on the mechanical properties is negligible and can be explained by a recovery process (either dynamic or static). In fact, a large grain size can evolve during plastic working, which is accompanied by a rapid recovery. The latter retards the accumulation of any excess dislocations at grain boundaries, thus inhibiting the development of high internal stresses. On the other hand, the effect of residual stresses on mechanical properties becomes significant with decreasing grain size. The additional strengthening due to internal stresses may be as much as 50% of the grain size strengthening when the grain size in severely deformed samples decreases to 100 nm.

5. Conclusions

Deformation microstructures have been studied and tensile tests carried out on an Fe–15%Cr ferritic stainless steel subjected to large-strain cold-working. The main results can be summarised as follows:

(1) Submicrocrystalline structures with a transverse grain size of ~200 nm can be developed in the steel samples by cold-rolling/swaging to a total strain of 4.6. After processing, the ultrafine grains are characterised by a relatively low dislocation density in grain/subgrain interiors and high residual stresses. The mean value of the internal stresses is ~0.2% of the shear modulus.

(2) The internal stresses result in complex elastic distortions of the crystal lattice in the strain-induced ultrafine grains. The most pronounced distortions were observed in vicinities of the grain/subgrain boundaries. The sources of high internal stresses were considered to be related to the local accumulation of excess grain boundary dislocations. Therefore, the grain/subgrain boundaries in severely deformed samples maintain high residual stresses.
(3) The high internal stresses significantly affect the mechanical properties of the submicrocrystalline samples in their as-processed state. The additional strengthening effect from strain-induced grain/subgrain boundaries bearing high internal stresses can reach approximately 50% of conventional grain size strengthening.
(4) The high internal stresses can almost be fully released by a light annealing treatment, which does not lead to any significant changes in the submicrocrystalline structures. The heat-treated samples, which have the same grain size in their submicrocrystalline structures as the cold-worked samples in the as-processed state, follow the ordinary Hall–Petch relationship.

Acknowledgements

The authors are grateful to J. Hono, National Institute for Materials Science, for improving the language of this article. A. Belyakov would like to thank the National Institute for Materials Science for providing a scientific fellowship.

References

[1] C. Suryanarayana, Int. Mater. Rev. 40 (1995) p.41.
[2] C.C. Koch, Nanostruct. Mater. 9 (1997) p.13.
[3] F.J. Humphreys, P.B. Prangnell, J.R. Bowen et al., Phil. Trans. R. Soc. Lond. 357 (1999) p.1663.
[4] R.Z. Valiev, R.K. Islamgaliev and I.V. Alexandrov, Prog. Mater. Sci. 45 (2000) p.103.
[5] Y. Wang, M. Chen, F. Zhou et al., Nature 419 (2002) p.912.
[6] C. Kobayashi, T. Sakai, A. Belyakov et al., Phil. Mag. Let. 87 (2007) p.751.
[7] I. Saunders and J. Nutting, Metal Sci. 18 (1984) p.571.
[8] Y. Iwahashi, Z. Horita, M. Nemoto et al., Acta Mater. 45 (1997) p.4733.
[9] A. Belyakov, W. Gao, H. Miura et al., Metall. Mater. Trans. A 29 (1998) p.2957.
[10] N. Tsuji, S. Okuno, Y. Koizumi et al., Mater. Trans. 45 (2004) p.2272.
[11] A. Belyakov, T. Sakai, H. Miura et al., Phil. Mag. A 81 (2001) p.2629.
[12] Yu. Ivanisenko, W. Lojkowski, R.Z. Valiev et al., Acta Mater. 51 (2003) p.5555.
[13] O. Sitdikov, T. Sakai, A. Goloborodko et al., Phil. Mag. 85 (2005) p.1159.
[14] A. Belyakov, Y. Kimura and K. Tsuzaki, Acta Mater. 54 (2006) p.2521.
[15] A. Belyakov, K. Tsuzaki, Y. Kimura et al., Mater. Sci. Eng. A 456 (2007) p.323.
[16] A. Belyakov, T. Sakai, H. Miura et al., Phil. Mag. Lett. 80 (2000) p.711.
[17] A. Belyakov, K. Tsuzaki, Y. Kimura et al., J. Mater. Res. 22 (2007) p.3042.
[18] A. Belyakov, T. Sakai, H. Miura et al., Scripta Mater 42 (2000) p.319.
[19] T. Shimokawa, T. Kinari and S. Shintaku, Phys. Rev. B 75 (2007) p.144108.
[20] A.E. Romanov and V.I. Vladimirov, *Disclinations in Crystalline Solids*, in *Dislocation in Solids*, Vol. 9, F.R.N. Nabarro, ed., Elsevier, Amsterdam, 1992, p.191.
[21] E.O. Hall, Proc. Phys. Soc. B 64 (1951) p.747.
[22] N.J. Petch, J. Iron Steel Inst. 174 (1953) p.25.
[23] R. Armstrong, I. Codd, R.M. Douthwaite et al., Phil. Mag. 7 (1962) p.45.

[24] Y. Bergstrom and H. Hallen, Metal Sci. 17 (1983) p.341.
[25] A.S. Khan, S.S. Yeong, X. Chen et al., Int. J. Plast. 22 (2006) p.195.
[26] M. Dao, L. Lu, R.J. Asaro et al., Acta Mater. 55 (2007) p.4041.
[27] L.L. Shaw, A.L. Ortiz and J.C. Villegas, Scripta Mater. 58 (2008) p.951.
[28] H.J. Frost and M.F. Ashby, *Deformation Mechanism Maps*, Pergamon Press, Oxford, 1982.
[29] D.R. Lesuer, C.K. Syn and O.D. Sherby, Mater. Trans. 47 (2006) p.1508.